available at www.sciencedirect.com

ScienceDirect

journal homepage: www.elsevier.com/locate/jmbbm

Research paper

Correlation of the mechanical and structural properties of cortical rachis keratin of rectrices of the Toco Toucan (*Ramphastos toco*)

S.G. Bodde[a], *M.A. Meyers*[a,b], *J. McKittrick*[a,b,*]

[a] *Materials Science and Engineering Program, University of California, San Diego, La Jolla, CA 92093-0418, United States*
[b] *Department of Mechanical and Aerospace Engineering, University of California, San Diego, La Jolla, CA 92093-0411, United States*

ARTICLE INFO

Article history:
Published online 4 February 2011

Keywords:
Feather
Tensile strength
Young's modulus
Weibull distribution
Avian keratin

ABSTRACT

Mechanical characterization of the cortex of rectrices (tail feathers) of the Toco Toucan (*Ramphastos toco*) has been carried out by tensile testing of the rachis cortex in order to systematically determine Young's modulus and maximum tensile strength gradients on the surfaces and along the length of the feather. Of over seventy-five samples tested, the average Young's modulus was found to be 2.56 ± 0.09 GPa, and maximum tensile strength was found to be 78 ± 6 MPa. The Weibull modulus for all sets is greater than one and less than four, indicating that measured strength is highly variable. The highest Weibull moduli were reported for dorsal samplings. Dorsal and ventral surfaces of the cortex are both significantly stiffer and stronger than lateral rachis cortex. On the dorsal surface, cortex sampled from the distal end of the feather was found to be least stiff and weakest compared to that sampled from proximal and middle regions along the length of the feather. Distinctive fracture patterns correspond to failure in the superficial cuticle layer and the bulk of the rachis cortex. In the cuticle, where supramolecular keratinous fibers are oriented tangentially, evidence of ductile tearing was observed. In the bulk cortex, where the fibers are bundled and oriented longitudinally, patterns suggestive of near-periodic aggregation and brittle failure were observed.

1. Introduction

Feathers are the most distinguishable feature of all modern birds, and they are considered to be the most complex integumentary appendages of all vertebrata (Lucas and Stettenheim, 1972). Feathers and all components are comprised of β-keratin; therefore, morphological and structural adaptations are expected to be the source of any variability in function and performance. The diversity of types of feathers, from structurally simple rictal bristles, which are analogous to eyelashes and whiskers of mammals (Lederer, 1972), of perching birds to the double shafted contour feathers of emus, exemplifies the degree of specialization in structure.

The contour feathers of birds capable of flight must be lightweight, sufficiently strong to withstand aerodynamic loads experienced during flight, and resistant to

* *Corresponding author at:* Department of Mechanical and Aerospace Engineering, University of California, San Diego, La Jolla, CA 92093-0411, United States. Tel.: +1 858 534 5425; fax: +1 858 534 5698.
E-mail address: jmckittrick@ucsd.edu (J. McKittrick).

1751-6161/$ - see front matter © 2011 Elsevier Ltd. All rights reserved.
doi:10.1016/j.jmbbm.2011.01.010

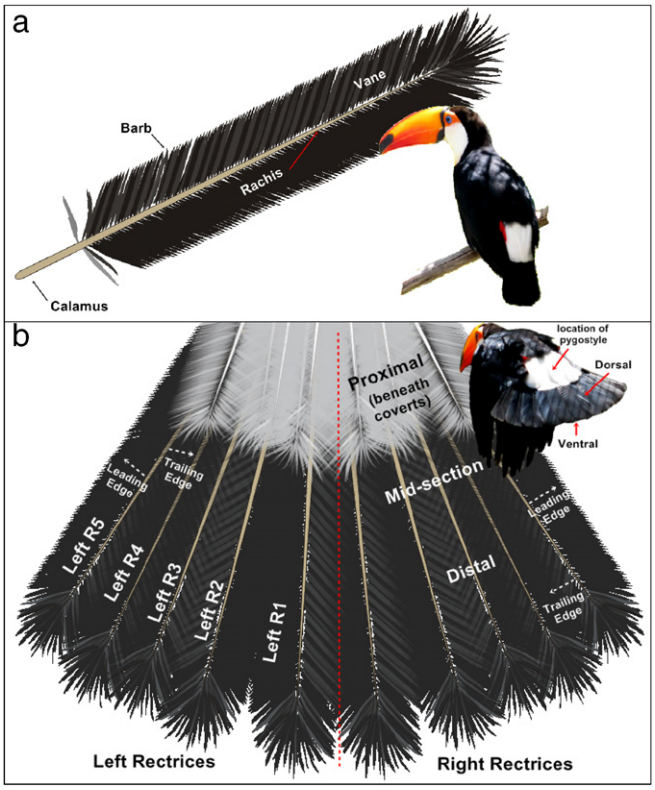

Fig. 1 – Schematic diagram of (a) rectrix or tail feather and (b) the tail of the Toco Toucan (*Ramphastos toco*) designates the outer to inner rectrices by index; the configuration of the right rectrices mirrors the order of the left rectrices. On the right, the proximal, middle, and distal sections are denoted. The trailing edge is the lateral surface facing the midline. The leading edge is the lateral surface facing away from the midline. Photographic inserts depict the Toco Toucan (a) in perching position and (b) in flight.

wear-induced damage, as they, unlike other keratinous integumentary structures which are continuously growing (e.g. talons/claws and the sheath of the bill), are replaced only periodically (semiannually to biannually) during molting (Gill, 1994). Toucans molt their tail feathers annually starting from the feathers at the center of the tail outward (Sedgwick, 2010).

The feather exemplifies a branched or hierarchical construction based on a primary shaft, or rachis consisting of a cortex that encloses a cellular core (Rutschke, 1966). The rachis, except at the bare calamus (the hollow base or quill which extends from the follicle) supports barbs, secondary keratinous features forming the herringbone pattern of the vane (Fig. 1(a)). The barbs, similarly support tertiary features or barbules. Structural hierarchy at the microscale has been revealed in the cortex of the rachis as well as of the barbs by means of microbe-assisted disassembly (Lingham-Soliar, 2009). In feathers that had been subjected to selective fungal degradation, it was revealed that the bulk of the cortex is constructed of fibers, measuring 6 μm in diameter, predominately aligned along the length of the shaft. Lingham-Soliar et al. (2009) claimed that these fibers are syncytial barbules, or multiple barbule cells connected end-to-end. These fibers are assembled of fibrils measuring 300–500 nm in diameter. The most superficial layer (cuticle) of the cortex is distinguishable from the bulk of the cortex in that it consists of circumferentially oriented fibers (Earland et al., 1962a,b). Earland et al. (1962a,b) reported that in the wing feather of a domestic goose, this cuticle comprised one-seventh of the thickness of the rachis at the calamus and decreased in thickness along the length of the rachis. Therefore, the feather can be described as a paradigm of a sandwich-structured composite (Crenshaw, 1980) and the cortex itself is a hierarchical, bi-laminate, fiber-reinforced composite.

While feather structure and microstructure have been studied previously (Lingham-Soliar et al., 2009; Filshie and Rogers, 1962; Chernova, 2005), work on mechanical properties of feather keratin has been scant in the literature and with inconsistent results. Due to the complex construction of feathers, a piecewise approach to understanding mechanical response of the feather has been adopted. The morphology, (e.g. cross-sectional geometry or microscopic attributes) of the cortex dominates bending behavior of the intact feather (Purslow and Vincent, 1978). The Young's modulus range for cortical rachis as reported in the literature from 1966 to 1980, encompasses nearly three orders of magnitude of variation (Bonser and Purslow, 1995). This is surprising considering that molecular properties of β-keratins suggest that they are biochemically similar (Brush and Wyld, 1982), and the molecular packing and filament framework is common across various avian keratins (Fraser and Parry, 2008). The variability in Young's modulus may be attributed to differences in testing and sampling procedures. Furthermore, considering that feather protein heterogeneity is prescribed at the genetic

level and that macro- and supramolecular interactions are affected by environmental and developmental constraints (Brush and Wyld, 1982), differences in physical properties of feathers collected from different species or even from different feather tracts of a single host of a particular species cannot be dismissed *a priori*.

Some attempts to identify interspecific variations in Young's modulus of rachis keratin sampled from the dorsal surface of the cortex have been reported in the literature. Bonser and Purslow (1995) tested cortex strips excised from the proximal (just after the calamus) region of the rachis on three outermost wing feathers sampled from eight species of birds. Based on tension testing, they reported that the interspecific variations in mechanical properties were low. The mean Young's modulus of the feather cortex was found to be 2.50±0.06 GPa and with few exceptions, the interspecific differences were not statistically significant. The mass of the species studied represents a range of almost three orders of magnitude (0.06–10 kg); therefore, the authors reported that the stiffness of the cortex does not vary with mass of the bird. Previously, MacLeod (1980) had tested segments of intact rachis (rachis segments in which the medullary core had not been separated from the cortex) from three species of landfowl and from a Herring Gull. In contrast to the conclusion reported by Bonser and Purslow (1995), for both tension and flexure, the interspecific variation in Young's modulus was high; for cortex from which the medulla had been removed, the tensile Young's modulus ranged from 1 to 8 MPa, where uncertainty was reported as ~10% (MacLeod, 1980). The discrepancy in the literature may be a result of differences in sampling technique, treatment, and environmental conditions (e.g. the mechanical performance of feather is reported to be humidity sensitive Bonser and Farrent, 2001; Taylor et al., 2004), although interspecific microstructural variation may play a role.

Significant intra-specific differences were identified as a function of position along the length of the rachis (Bonser and Purslow, 1995; MacLeod, 1980; Bostandzhiyan et al., 2006). The distal (furthest from body) region of the feather is more mature than the proximal region (closest to body), and morphology is substantially different along the length (Prum, 1999), in terms of size, cross-sectional geometry, and thickness of the cuticle (Earland et al., 1962a,b). This was reported in cortical rachis along a single wing feather of a Mute Swan, one of the most massive of the flying species of birds (Bonser and Purslow, 1995). The Young's modulus from the proximal end to the distal tip, based on tension testing of dorsal (top surface of feather rachis) cortex strips, was found to increase linearly, from 1.8 to 3.8 GPa (Bonser and Purslow, 1995). In the study by MacLeod (1980), the Young's modulus values of the distal end of a given species, in the range from 210–682 MPa systematically exceeded those for the proximal end, reported to be from 45–180 MPa for the same species. This trend was reported to be absent in the rachis of the flightless ostrich (Cameron et al., 2003). Bostandzhiyan et al. (2006) reported failure strength of dorsal sections of cortex collected from a goose to be 188–240 MPa at the calamus and 74 MPa at a more distal section, while Weiss and Kirchner (2010) reported an inverse trend for the tail coverts of a wild-type peacock, a generally cursorial (running) species. Therefore, for birds capable of flight, temporal effects and fiber alignment gradients from the proximal to distal end may contribute to an increase of at least 100% in stiffness or a decrease in failure strength by more than 200%.

The objective of this research is to systematically characterize rachis cortex from the tail feathers of the Toco Toucan (*Ramphastos toco*) in tension and to correlate mechanical properties with such variables as surface location and distance along the rachis. In doing so, it is possible to correlate Young's modulus and maximum tensile strength with respect to position on feather and location of feather on the tail. A secondary objective of this study is to observe the fracture pattern. Based on ecology of the species, it is anticipated that the rectrices of the Toco Toucan, being a scansorial species who uses the tail for support during tree-climbing, might be stiffer than those of other species, but this effect is speculated to be dependent on cross-sectional size and geometry effects (Tubaro et al., 2002).

2. Materials and methods

2.1. Material acquisition and handling

All ten rectrices (Fig. 1), five on each side of the pygostyle (the ossified vertebrae which support the tail feathers) were extracted from a single donor toucan. The toucan specimen was acquired from Emerald Forest Bird Gardens in Fallbrook, California after death by unknown causes in captivity and stored frozen until the time of sample preparation. Freezing was enacted in order to arrest or prevent any effects of microbial degradation. Unfortunately, the authors know nothing of the age or molt stage. Based on the average length of rectrices, measured to be 17.3 ± 0.3 cm, there is reason to speculate that the specimen was a male (female tail length ranges from 14.2 to 16.2 cm and male tail length is from 14.1 to 17.9 cm) (Sedgwick, 2010). Prior to sample preparation, imaging, and mechanical testing, the sections of material were removed from the specimen and stored in a desiccator at room temperature for at least 24 h. Whether or not freezing, thawing, and desiccation affects structure significantly so as to affect material properties is unknown at this point.

2.2. Electron microscopy

The microstructure of the cortical rachis and fracture surfaces were imaged using either a FEI Quanta 600 Scanning Electron Microscope (SEM) or a Phillips XL30 environmental SEM. All samples were coated with gold/palladium or chromium alloy. Preserved microstructure of feather rachis was prepared for imaging by means of a freeze fracture technique in which the sample was manually fractured after being submerged in liquid nitrogen.

2.3. Tensile sample preparation

The ten rectrices (Fig. 1(b)) were stripped of the barbs and sectioned into segments of approximately 5 cm in length. Dorsal, ventral, and lateral surfaces of the rachis cortex,

separated from the medullary core, from three regions along the length of the feather were excised for testing. The cortex ranged in thickness from 0.07 to 0.63 mm, and the width of excised samples measured from 0.33 to 2.74 cm, the thinnest and most narrow of which were sampled from the lateral surfaces of the rachis. The termini of the approximately rectangular strips were shielded in aluminum sheets affixed by cyanoacrylate adhesive, leaving a test gauge length of 10.11 ± 0.05 mm ($N = 83$). The samples were extended in tension using an Instron (Model No. 3347) testing apparatus. All samples were tested at a nominal strain rate of 1.88×10^{-3}/s, which based on previous work on avian keratins by Seki et al. (2005), is in the regime of ductile pull-out failure and near the anticipated threshold of brittle failure. The most proximal region was within 6 cm of the calamus. Samples taken from the middle section were within 10 cm of the calamus. The most distal samples were taken from within 10 to 15 cm of the calamus, beyond which cortex samples were too thin for reliable cutting and handling. Stress–strain data were computed from force–extension curves acquired from machine interface software and sample dimension measurements. The data were analyzed using LabVIEW software in order to compute maximum stress and maximum Young's modulus with a capped variance. The maximum slope on the stress–strain curve was taken to be Young's modulus, the maximum stress was taken as the tensile strength.

3. Theory/calculations

Best estimates for both the Young's modulus (Dey et al., 2009) and tensile strength were determined by fitting for the scale and shape parameters of the Weibull cumulative distribution function for each sampling set:

$$F_V(x_i;\alpha,m) = 1 - \exp\left[-V_i\left(\frac{x_i}{\alpha}\right)^m\right],$$

where $F_V(x_i;\alpha,m)$ is the probability that the Young's modulus or the fracture strength has a value less than x_i. The variable x_i is the measured Young's modulus or fracture strength, and α is the scale or statistical dispersion parameter for either the set of values for Young's modulus or for fracture strength, respectively. The shape parameter or stretching exponent, m, for the case of maximum strength data is defined as the Weibull modulus. By plotting $\ln[-\ln(1-F_V(x_i))]$, where $F_V(x_i)$ is determined by mean rank method, against $\ln x_i$, the shape and scale parameters were determined by linear fitting. From the respective fitting parameters, the mean, μ, and standard deviation, σ_μ, for both strength and Young's modulus were computed for a nominal volume according to:

$$\mu = \frac{\alpha}{V^{1/m}}[\Gamma(1+1/m)];$$

$$\sigma_\mu = \left(\frac{\alpha}{V^{1/m}}\right)^2 \sqrt{\Gamma(1+2/m) - \Gamma^2(1+1/m)}.$$

4. Results and discussion

4.1. Structure of the feathers

The meso-structure and cross-section of a contour feather are shown in Fig. 2. The rachis consists of a thin cortex (249 ± 12 μm), which encloses a relatively thick cellular core (measuring from 600 μm to a few millimeters in diameter) similar to a sandwich structured composite (Fig. 2(a)). This design satisfies resistance to flexure and rupture during flexure without a proportionate increase in weight (Crenshaw, 1980). The SEM images of dorsal (Fig. 2(b)) and ventral (Fig. 2(c)) surfaces reveal relatively smooth topography compared to that of lateral surfaces (Fig. 2(d)) which exhibit intersecting ridges with a spacing at 10 μm–20 μm, with considerable overlap with diameter of cells of the medullary core (Fig. 2(e)) ranging from 20 μm to 30 μm. The smoothness, at microscale, of the dorsal and ventral surfaces is remarkable, as it is expected that surface roughness would serve to decrease drag (i.e. if the laminar-to- turbulent transition occurs before the point of boundary layer separation), as proposed regarding microscale features observed on the surface of barbs (Chernova, 2005).

The cortex also incorporates fiber-reinforcement in the design. Freeze-fracture (Fig. 3) reveals the cross-section of axially-aligned fibers, measuring 6–9 μm in diameter, similar in dimensions to those reported by Lingham-Soliar et al. (2009). The fibers are constructed of fibril bundles measuring 250–600 nm, again similar to the dimensions of supramolecular β-keratin fibril bundles reported by Lingham-Soliar et al. (2009). Therefore, the fibrous construction in the bulk of the rachidial cortex is hierarchical in itself.

4.2. Mechanical characterization

Typical stress–strain curves are plotted in Fig. 4. As shown, there is considerable variability in mechanical properties. Most dorsal and ventral samples failed at strains higher than 5% and some even in excess of 10%, while the majority of lateral samples failed at less than 5% strain. With a large sample size (see Table 1 for number of samples tested), Weibull statistical analysis can be applied. The Weibull modulus in all cases of this study is greater than one and less than four; therefore, variability in strength is high, as can be expected for organic, natural materials, and comparable to that of traditional whiteware and structural ceramics. The volume dependence in Young's modulus and strength over the range of sample volumes (0.24–14 mm^3) suggests that the sample size is not sufficiently larger than the critical size of meso-structural features that dominate tensile behavior.

Weibull probability plots for Young's modulus and failure strength data are shown in Figs. 5–7. The samples excised from the left rectrices demonstrate marginally higher stiffness with lower Weibull modulus than those from the right rectrices (Table 1). It has been reported that among parrots observed in captivity, left-handedness (or rather left-footedness, in the sense that parrots use their feet to manipulate toys or food) is prevalent (Friedmann and Davis, 1938). Another possible explanation would be route preference. The rectrices are enacted as a rudder during flight, and the feathers are fanned during landing. If, for example, the individual preferred clockwise trajectories, longitudinal aeroelastic stress would be greater for the left side of the tail.

Samples of dorsal and ventral cortex were found to be significantly stiffer and stronger than those of the lateral edges (Figs. 5 and 6(b)). Samples from the dorsal surface sustain both the highest stress and the highest stiffness. While having similar strength, relative to lateral surfaces,

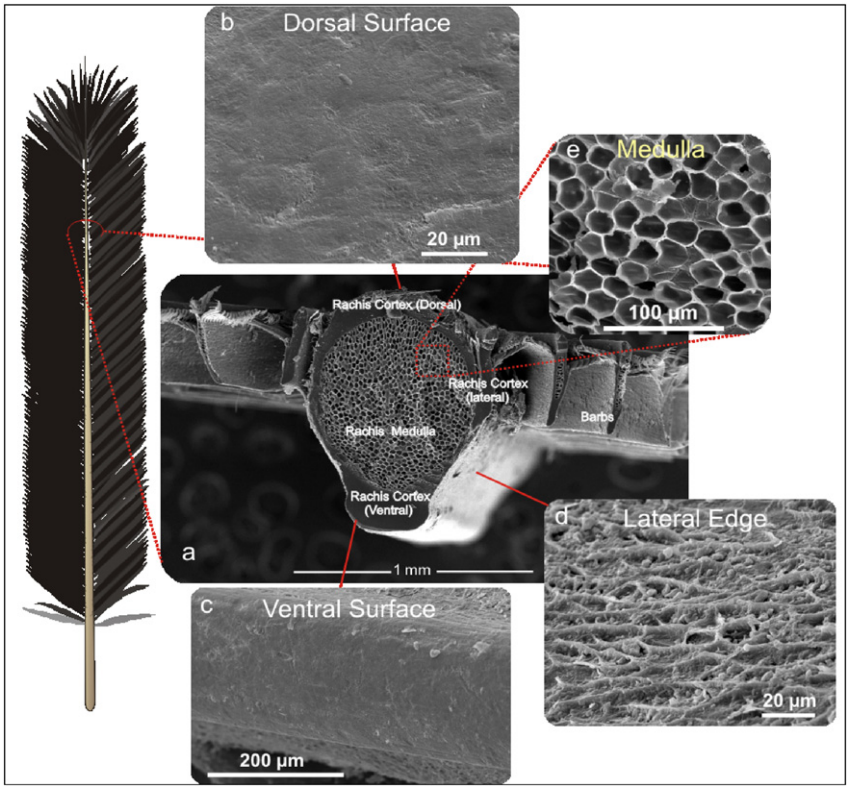

Fig. 2 – SEM of the surface microstructure of the cortex and (a) the cross-section of a distal section of rachis. The (b) dorsal and (c) ventral cortical rachis is smooth at the microscale, while the (d) lateral cortical rachis keratin is fibrous and textured with ridges separated by 10–20 μm. The cortex encloses (e) a medullary core constructed of cells ranging from 20–30 μm in diameter.

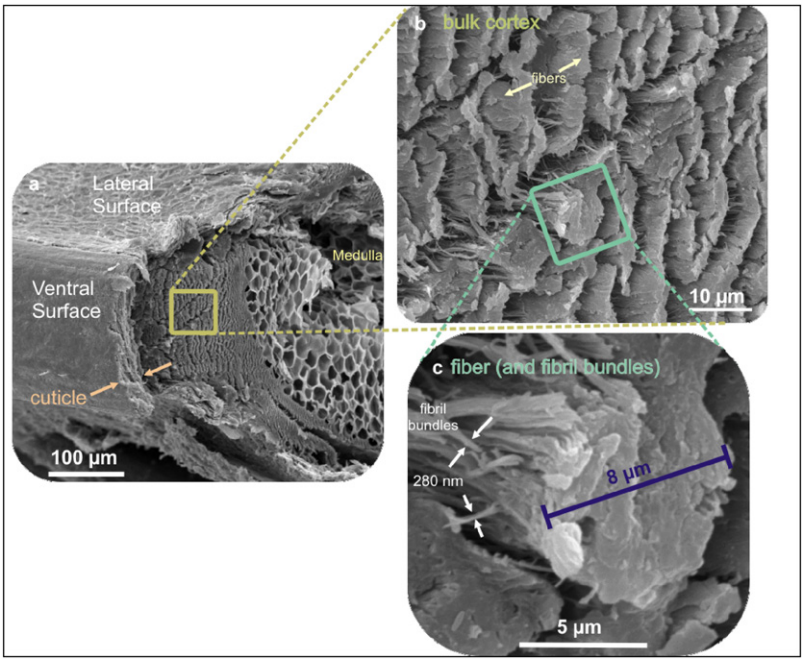

Fig. 3 – SEM of the cross-sectional cortex microstructure. Freeze fracture of distal rachis reveals (a) the ventral cuticle and (b) the ventral bulk cortex in which fibers measuring 6–9 μm in diameter run longitudinally. These features are similar in dimension as those reported by Lingham-Soliar et al. (2009). (c) These microscale fibers are constructed of bundles of fibrils measuring 250–600 nm in thickness, again matching the order of magnitude in thickness of the fibrillar assemblies observed by Lingham-Soliar et al. (2009).

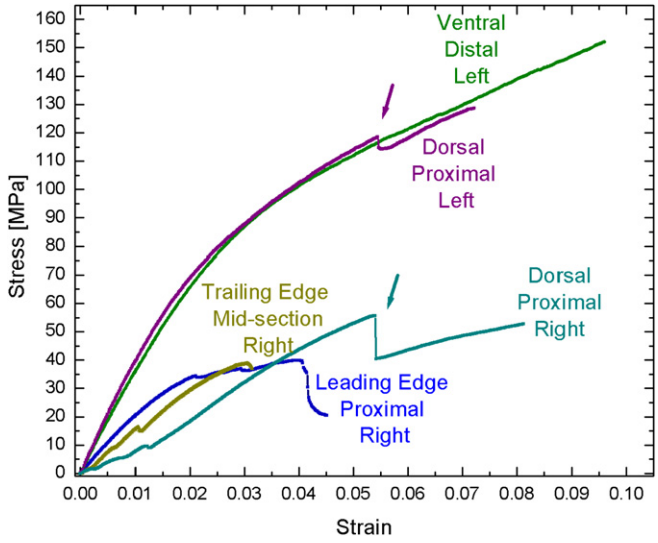

Fig. 4 – Typical tensile stress–strain curves for cortical rachis keratin. Rachis cortex sampled from dorsal and ventral surfaces exhibits linear elasticity over a larger strain range than lateral samples. Arrows denote localized failures. Variation in stiffness and maximum tensile strength is high.

Table 1 – Summary of tensile properties of cortical rachis keratin excised from rectrices of the Toco Toucan (*Ramphastos toco*). The Young's Modulus ($\bar{E}$) and maximum strength ($\bar{\sigma}$) of all samples of the set are represented the Weibull mean using nominal volume, 4.06 mm^3 (mean volume for all samples in this study) where the uncertainty is the standard error of the mean as computed from the Weibull probability plot fitting parameters. The stretching exponent, m_E, is that associated with the Young's modulus distribution and m_σ is the Weibull modulus. The location of R1–R5 is depicted in Fig. 1(b).

Criterion	Samples	$\bar{E}$ (GPa)	m_E	N_E	$\bar{\sigma}$ (MPa)	N_σ	m_σ
	All samples	2.56 ± 0.09	3.60 ± 0.15	81	78 ± 6	76	1.61 ± 0.09
Side of tail	Left	2.65 ± 0.15	3.14 ± 0.23	40	77 ± 10	37	1.28 ± 0.11
	Right	2.47 ± 0.12	3.7 ± 0.3	41	79 ± 7	39	1.88 ± 0.15
Rachis surface	Dorsal	2.99 ± 0.15	4.24 ± 0.19	28	118 ± 8	28	3.15 ± 0.21
	Ventral	2.82 ± 0.17	3.63 ± 0.25	26	78 ± 10	22	1.71 ± 0.19
	Leading Edge	1.96 ± 0.17	3.2 ± 0.3	15	40 ± 7	15	1.59 ± 0.24
	Trailing Edge	1.86 ± 0.15	3.9 ± 0.8	12	33 ± 5	11	2.3 ± 0.5
Distance along the rachis	Proximal	2.57 ± 0.11	4.7 ± 0.4	27	78 ± 9	31	1.67 ± 0.18
	Mid-section	2.54 ± 0.18	2.78 ± 0.18	29	84 ± 13	27	1.25 ± 0.13
	Distal	2.48 ± 0.21	3.01 ± 0.26	19	75 ± 12	18	1.5 ± 0.3
Rectrix index (inner to outer)	R1	2.51 ± 0.20	3.4 ± 0.3	17	88 ± 18	15	1.29 ± 0.15
	R2	2.35 ± 0.22	2.8 ± 0.4	18	83 ± 18	16	1.16 ± 0.27
	R3	2.76 ± 0.20	4.2 ± 0.5	15	72 ± 13	18	1.31 ± 0.19
	R4	2.28 ± 0.15	4.0 ± 0.5	18	90 ± 17	13	1.51 ± 0.20
	R5	2.95 ± 0.33	2.7 ± 0.5	13	80 ± 14	13	1.6 ± 0.4
For comparison	Proximal-Dorsal	3.14 ± 0.28	4.04 ± 0.28	10	125 ± 15	10	3.0 ± 0.3
	Mid-Dorsal	3.2 ± 0.4	3.21 ± 0.22	8	141 ± 23	8	2.33 ± 0.11
	Distal-Dorsal	2.69 ± 0.25	3.9 ± 0.3	10	99 ± 10	10	3.5 ± 0.4

dorsal and ventral cortex differ substantially in Weibull modulus. Dorsal samples have the highest Weibull modulus of tensile strength compared to any other sample groupings, implying that the variability in the distribution of the flaws is lower than for other samplings. The discrepancy in mechanical properties on the surfaces of the cortex may be related to the role of melanin, a pigment macromolecule that provides the black coloration in plumage in the form of rod-like granules (Filshie and Rogers, 1962). The dorsal surface appears to be uniformly and densely melanized; the ventral surface, based on visual inspection, is less melanized, appearing brown in color in some places, and the lateral surfaces are non-melanized. Bonser (1995) reported a 39% increase in microhardness of melanized dorsal cortex from the wing feather of a ptarmigan compared to non-melanized ventral surfaces. The discrepancies in Weibull modulus and in strength of dorsal and ventral samples may be correlated with melanin distribution in those surfaces.

Distal samples of cortical rachis were weakest and least stiff compared to proximal and middle specimens, but

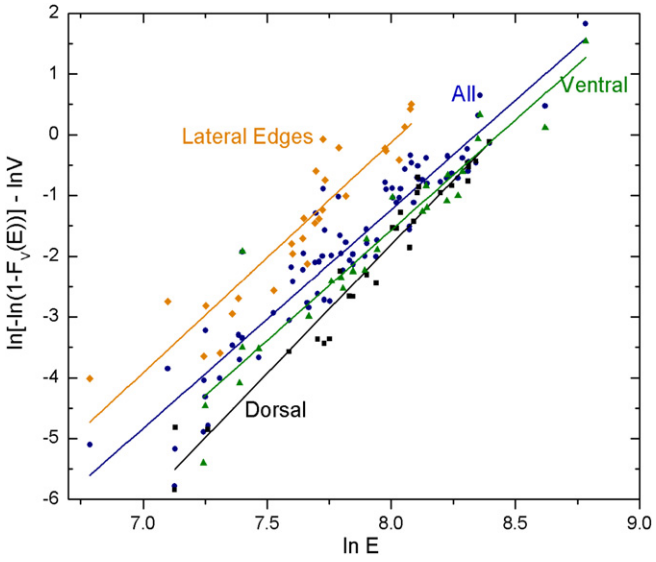

Fig. 5 – Weibull probability plot for Young's modulus data of all samples against data sorted by surface from which the rachidial cortex was collected. The maximum Young's modulus for each sample in the set is plotted along with the fitting result (solid line). The stiffness of dorso-ventral cortex is significantly greater than that for lateral samples.

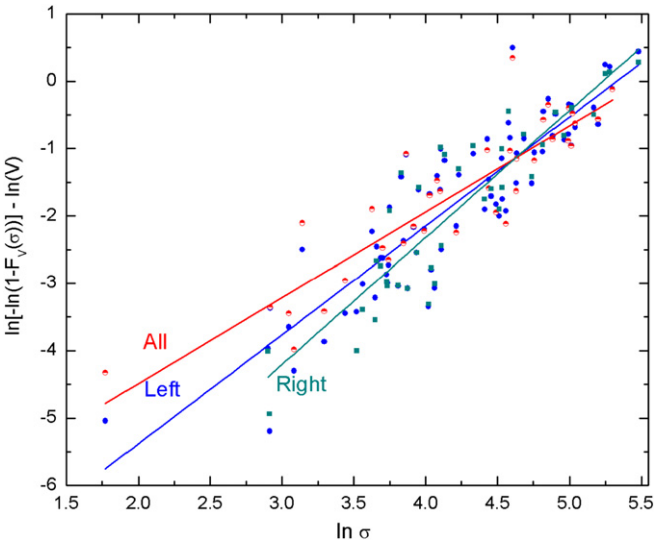

Fig. 6 – Weibull probability plot of tensile strength of rachidial cortex with respect to position on the tail. Maximum tensile stress for each sample is plotted against the fitted Weibull distribution function (lines). Cortical rachis samples excised from right rectrices are marginally stronger than those from left rectrices.

not significantly so. The fracture strength and stiffness of proximal and middle specimens were approximately equivalent. This result is in contrast to the proximal to distal increase in stiffness reported by Bonser and Purslow (1995) for the case of the wing feathers of the swan and suggested to be correlated to the increased proportion of the axially oriented fibers in the cortex. An increasing stiffness gradient from proximal to distal end may serve to compensate for the effect of decreased cross-sectional area along the length of the feather, if flexural stiffness, *EI*, where *I* is the second moment of inertia, is to be conserved or compensated. However, this gradient in strength and stiffness may be confounded by a temporal or aging effect of keratin, as the more distal cortex is more mature (Prum, 1999). The cortex sampled from distal regions of peacock tail coverts was significantly less crystalline than in other regions along the length of the feather (Pabisch et al., 2010). Therefore, the cortex of the rachis, in addition to being a fiber-reinforced bi-laminate composite, may also be described as functionally graded. Whether or not proximal to distal age effects are significant relative to confounding effects of molt cycle (i.e. feathers at the end of the annual molt cycle may be micro-structurally and mechanically different than those recently re-grown) is not revealed by this study.

The stiffness of the dorsal-proximal cortex was found to exceed the values reported by Bonser and Purslow

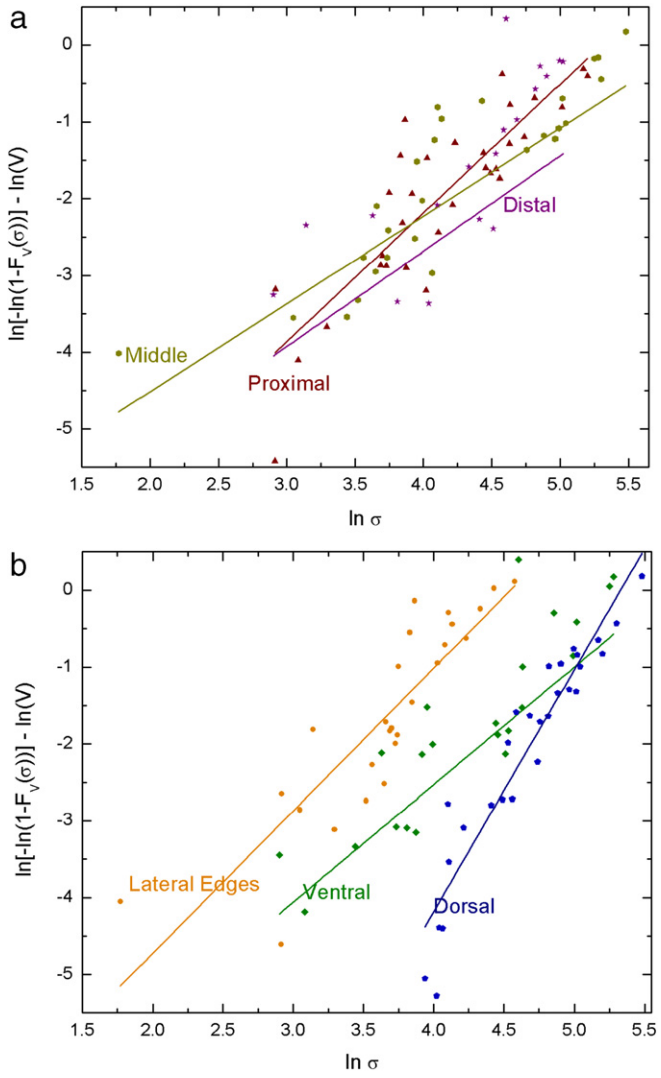

Fig. 7 – Weibull probability plots of tensile strength of the cortex with respect to location on the rachis. Maximum tensile stress data are grouped according to (a) region along the rachis and (b) surface on the rachis. (a) The proximal, middle, and distal regions did not reveal any significant trends in strength or Weibull modulus along the length of the feather. (b) When maximum tensile strength data are grouped according the rachis surface, dorso-ventral cortex is significantly stronger than lateral cortex. The dorsal surface exhibits the highest strength as well as the highest Weibull modulus.

(1995) for samples from wing feathers of other avian taxa. Noteworthy is that toucans are of the same taxonomic order as woodpeckers, who are believed to have stiffer rectrices (Burt, 1930). As they both nest in tree-cavities, woodpeckers and toucans are considered to be climbing birds. The Young's modulus determined for proximal-dorsal cortex of toucan retrices, 3.14 ± 0.28 GPa, is significantly greater than values reported by Bonser and Purslow (1995) (the mean of which was 2.50 ± 0.06 GPa). The comparison of the cortex from tail feathers to wing feathers may be inappropriate; however considering that feathers involved in flapping are expected to be more flexible, the skew in the comparison would favor the hypothesis that cortical rachis of toucan rectrices would be stiffer. Therefore, further studies are necessary in order to conclude whether or not higher stiffness measured for toucan rectrices holds true for scansorial species or for rectrices of all species.

Fracture surfaces

The fibrous and hierarchical structure of the cortical rachis was further revealed by the tensile fracture surfaces. The fractures were generally compound, involving both brittle and ductile failure regimes (Fig. 7). The superficial cortical failure regime is easily distinguishable from the region of the longitudinal fiber fracture. The longitudinally oriented fibers revealed by Lingham-Soliar et al. (2009) to be syncytial barbules cleave in a brittle fashion, while the more superficial, tangentially oriented fibers at the cuticle seem to fail by ductile tearing. From the delaminated dorsal surface, microcracks are observed along the longitudinal axis and between fibers (Fig. 8(b)). Microcracks observable in the cross-section are oriented radially (Fig. 8(d)). This may be evidence of a Cook and Gordon (1964) crack blunting mechanism in which the crack initiated in the plane normal to the direction

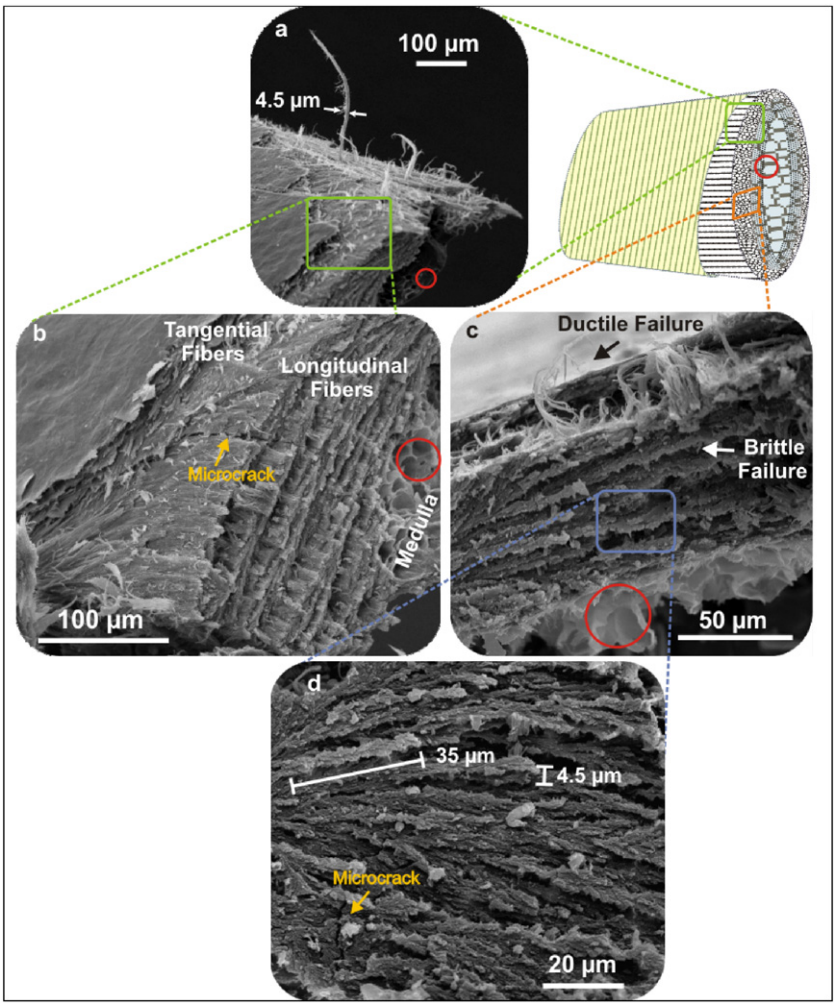

Fig. 8 – Cortical rachis fractured in tension imaged by SEM. The (a) fracture surface exhibits two domains of surface characteristics (b) viewable with respect to the dorsal surface and (c) at the cross-section: the superficial region exhibiting ductile failure behavior of the fibers as well as separation of bundled fibrils (circles indicate residual medulla) and a (d) bulk region exhibiting brittle cleavage of what appears to be a laminate composite consisting of near-periodic and staggered assemblies measuring 40–50 μm in arc length along the circumference and 4–7 μm in thickness.

of uniaxially applied stress is deflected and redirected along interfibrous paths oriented along the longitudinal axis (Fig. 8).

Also observable in the fracture surface of the bulk cortex are staggered, near-periodic domains, tangentially-striated in the bulk cortex (Fig. 8(c)–(d)), measuring 35–40 μm in length, and comparable in thickness to the diameter of the fibers observed in freeze fractured cortex at 4–7 μm. This microstructure has not been described previously in the literature, and it may be evidence of a stress-induced reorganization of the longitudinally-oriented fiber bundles in the bulk cortex in order to accommodate failure strains as high as 10% (Fig. 4).

5. Conclusions

Significant conclusions of this study include:

- Using Weibull probability analysis, the average tensile stiffness of the rachis cortex of the tail feathers of the Toco Toucan (*Ramphastos toco*) is 2.56±0.09 GPa, and tensile strength is 78 ± 6 MPa.
- The Weibull modulus of all sample groupings is greater than one and less than four. The equivalent stretching parameters resulting from fitting of Young's modulus data ranges from two to eight indicating that for some sample groupings, the Young's modulus is a more reliable material parameter than maximum strength.
- Dorsal and ventral cortex samples are both stronger and stiffer than lateral cortex samples. Dorsal samples were stronger and significantly stiffer than ventral samples.
- No significant trend in stiffness or strength from the proximal to distal regions along the length of the feather were observed after correcting for sample volume.
- The Young's modulus of dorsal proximal rachis cortex samples as reported in this study are significantly higher than those values for all species reported by Bonser and Purslow (1995).
- Fracture surfaces imaged by SEM reveal distinguishable patterns in the cuticle and in the bulk of the cortex. Fibers

of the cuticles appear to rupture by ductile failure, while the bulk cortex undergoes brittle failure.

- Radially oriented microcracks were observed in some fracture surfaces of cortex. The longitudinally oriented fibrillar bundles in the bulk of the cortex may serve to deflect these radial microcracks according to the Cook–Gordon mechanism, redirecting them axially along inter-fibrillar interfaces.

Acknowledgements

The authors thank Aruni Suwarnasarn of the analytical facility at Scripps Institution of Oceanography and Michael Clark and Ryan Anderson of Nano3 at the California Institute for Telecommunications and Information Technology for technical assistance with microstructural study of feather by SEM. The authors are grateful to Mr. Jerry Jennings of Emerald Forest Bird Gardens for his cooperation. This work was completed with the diligent assistance of Kevin Choi, Timothy Kim, Danny Ngo, and James Kiang. SGB thanks Dr. Yasuaki Seki for his valuable mentorship. Finally, this manuscript was significantly improved by the valuable and constructive criticism of an anonymous reviewer. This project is funded in part by National Science Foundation, Division of Materials Research, Biomaterials Program (Grant DMR 0510138) and Ceramics Program (Grant DMR 1006931).

REFERENCES

Bonser, R.H.C., 1995. Melanin and the abrasion resistance of feathers. Condor 95, 590–591.

Bonser, R.H.C., Farrent, J.W., 2001. Influence of hydration on the mechanical performance of duck down feathers. Br. Poult. Sci. 42, 271–273.

Bonser, R.H.C., Purslow, P.P., 1995. The Young's modulus of feather keratin. J. Exp. Biol. 198, 1029–1033.

Bostandzhiyan, S.A., Shteinberg, A.S., Bokov, A.V., 2006. Fiziko-mekanicheskie svojstva sterzhnya pitch'ego pera. Dokl. Akad. Nauk 408, 772–775.

Brush, A.H., Wyld, J.A., 1982. Molecular organization of avian epidermal structures. Comp. Biochem. Physiol. B Comp. Biochem. 73 (2), 313–325.

Burt, W.H., 1930. Adaptive Modifications in the Woodpeckers. Univ. Calif. Publ. Zool, Berkeley, CA.

Cameron, G., Wess, T., Bonser, R., 2003. Young's modulus varies with differential orientation of keratin in feathers. J. Struct. Biol. 143, 118–123.

Chernova, O.F., 2005. Polymorphism of the architectonics of definitive contour feathers. Dokl. Akad. Nauk 404, 280–285.

Cook, J., Gordon, J.E., 1964. A mechanism for the control of crack propagation in all-brittle systems. Proc. R. Soc. A 282, 508–520.

Crenshaw, D.G., 1980. Design and materials of feather shafts: very light, rigid structures. Sym. Soc. Exp. Biol. 34, 485–486.

Dey, A., Mukhopadhyay, A.K., Gangadharan, S., Sinha, M.K., Basu, D., 2009. Weibull modulus of nano-hardness and elastic modulus of hydroxyapatite coating. J. Mater. Sci. 44, 4911–4918.

Earland, C., Blakey, P.R., Stell, J.G.P., 1962a. Molecular orientation of some keratins. Nature 196, 1287–1291.

Earland, C., Blakey, P.R., Stell, J.G.P., 1962b. Studies on the structure of keratin. IV. The molecular structure of some morphological components of keratins. Biochem. Biophys. Acta 56, 268–274.

Filshie, B.K., Rogers, G.E., 1962. An electron microscope study of the fine structure of feather keratin. J. Cell Biol. 13, 1–12.

Fraser, R.D.B., Parry, D.A.D., 2008. Molecular packing in the feather keratin filament. J. Struct. Biol. 162, 1–13.

Friedmann, H., Davis, M., 1938. Left-handedness in parrots. The Auk. 55, 478.

Gill, F.B., 1994. Ornithology, 2nd ed. W.H. Freeman and Company, New York, NY.

Lederer, R.J., 1972. The role of avian rictal bristles. Wilson Bull. 84, 193–197.

Lingham-Soliar, T., Bonser, R.H.C., Wesley-Smith, J., 2009. Selective biodegradation of keratin matrix in feather rachis reveals classic bioengineering. Proc. R. Soc. B 277, 1161–1168.

Lucas, A.M., Stettenheim, P.R., 1972. Avian Anatomy—Integument. In: Agricultural Handbook, vol. 362. Government Printing Office, Washington, DC.

MacLeod, G.D., 1980. Mechanical properties of contour feathers. J. Exp. Biol. 87, 65–71.

Pabisch, S., Puchegger, S., Kirchner, H.O.K., Weiss, I.M., Peterlik, H., 2010. Keratin homogeneity in the tail feathers of pavo cristatus and pavo cristatus mut. alba. J. Struct. Biol. 172, 270–275.

Prum, R.O., 1999. Development and evolutionary origin of feathers. J. Exp. Zool. 285, 291–306.

Purslow, P.P., Vincent, J.F.V., 1978. Mechanical properties of primary feather from the pigeon. J. Exp. Biol. 72, 251–260.

Rutschke, E., 1966. Untersuchungen über die Feinstruktur des Schaftes der Vogelfeder. Zool. Jahr. Syst. 93, 223–288.

Sedgwick, C., 2010. Toco Toucan (Ramphastos toco). In: Schulenberg, T.S., (Ed.). Neotropical Birds Online Cornell Lab of Ornithology. Ithaca. Retrieved from neotropical birds online: http://neotropical.birds.cornell.edu/portal/species/overview?p_p_spp=302936.

Seki, Y., Schneider, M.S., Meyers, M.A., 2005. Structure and mechanical behavior of a toucan beak. Acta Mater. 53, 5281–5296.

Taylor, A.M., Bonser, R.H.C., Farrent, J.W., 2004. The influence of hydration on the tensile and compressive properties of avian keratinous tissue. J. Mater. Sci. 39, 939–942.

Tubaro, P.L., Lijtmaer, D.A., Palacios, M.G., Kopuchian, C., 2002. Adaptive modification of tail structure in relation to body mass and buckling in Woodcreepers. Condor 104, 281–296.

Weiss, I.M., Kirchner, H.O.K., 2010. The Peacock's train (Pavo cristatus and Pavo cristatus mut. alba) I. structure, mechanics, and chemistry of the tail feather coverts. J. Exp. Zool. 313A, 690–703.